7-25-2007

Exohedral silicon fullerenes: $Si_NPt_{N/2}$ ($20 \leq N \leq 60$)

Yong Pei
University of Nebraska - Lincoln, ypei2@unl.edu

Yi Gao
University of Nebraska - Lincoln, ygao3@Unl.edu

Xiao Cheng Zeng
University of Nebraska-Lincoln, xzeng1@unl.edu

Exohedral silicon fullerenes: $Si_NPt_{N/2}$ ($20 \leq N \leq 60$)

Yong Pei, Yi Gao, and X. C. Zeng[a)]
Department of Chemistry, University of Nebraska-Lincoln, Lincoln, Nebraska 68588 and Nebraska Center for Materials and Nanoscience, University of Nebraska-Lincoln, Lincoln, Nebraska 68588

(Received 9 April 2007; accepted 22 May 2007; published online 25 July 2007)

Using density functional theory method we show that hollow silicon fullerene cages, Si_N ($20 \leq N \leq 60$), can be fully stabilized by exohedrally coated platinum atoms ($Pt_{N/2}$), denoted as $Si_NPt_{N/2}$. The exohedral coating $Pt_{N/2}$ passivates the dangling bonds of the silicon cages, thereby making the silicon cages Si_N to retain the symmetry and structure of homologous carbon fullerenes C_N. In particular, the I_h symmetrical, 60-atom silicon buckminsterfullerene cage (Si_{60}) can be fully stabilized by exohedrally coated 30 Pt atoms. Properties of $Si_NPt_{N/2}$, such as the highest occupied molecular orbital-lowest unoccupied molecular orbital (HOMO-LUMO) gap and relative stability of cage isomers, are calculated and compared with their carbon counterparts. It is found that the HOMO-LUMO gaps of $Si_NPt_{N/2}$ are close to their carbon fullerene counterparts (C_N). The trend in relative stability for exohedral fullerene isomers $Si_NPt_{N/2}$ is similar to that for the homologous carbon fullerenes (C_N). The exohedral Pt coating offers a possible molecular design towards stabilizing the silicon fullerene cages.
[DOI: 10.1063/1.2749514]

INTRODUCTION

Fullerene refers to a class of hollow carbon spheroids, which is composed of a certain number of pentagonal and hexagonal rings.[1] Since the discovery of the buckminsterfullerene C_{60}, carbon fullerenes have been subjected to intensive studies.[2,3] The physical and chemical properties of C_{60} and other fullerenes have yielded many intriguing results.[1] Motivated by the discovery of carbon fullerenes, attempts have been made to seek alternative freestanding fullerene structures constructed by other elements.[4–6] An open question is whether silicon can form similar fullerene structure, since the silicon element is directly under the carbon in the Periodic Table.

Silicon and carbon both form diamond structure in bulk crystal and both have four valence electrons in the outer valence shell. However, an important difference between elemental silicon and carbon is that carbon can form sp^2 hybrid C═C double bond, whereas silicon does not.[7] The Si═Si π bond is relatively weak and has bent geometry rather than the planar structure like the C═C double bond.[7] Indeed, the Si═Si π bond can be viewed as a diradical structure.[7] Analogous to the dangling bond induced reconstructions of two-dimensional cleaved silicon surface, such as (111) and (001),[8] the abundant unsaturated dangling bonds on the silicon fullerene cages render the cage structure unstable. Rearrangements of skeleton silicon atoms are undoubtedly expected to reduce the number of dangling bonds on the cage surface. In fact, numerous theoretical and experimental evidences have shown that the low-lying medium-size silicon clusters do not form hollow cage structures.[9–12] Rather, they tend to form external puckered "stuffed-fullerene-like" structures for clusters larger than Si_{27}.[12]

Much effort has also been devoted to stabilizing the silicon fullerene structure.[11,13–19] However, evidence for "bucky silicon" is yet to be revealed in the laboratory. Progresses have been made in synthesizing certain forms of metal encapsulated silicon cage structures. For example, small silicon cages with a single metal atom encapsulated (e.g., $W@Si_{12}$, $Ti@Si_{16}$, and $Sc@Si_{16}$) have been detected in ionic trap,[13] mass spectrometry, and anion photoelectric spectroscopy experiments.[17] Moreover, a palladium dimer encapsulated deltahedron germanium cage, $Pd_2@Ge_{18}^{4-}$, has been synthesized recently.[20] Strictly speaking, however, these cages are not conventional-fullerene-like since the cages are composed of trigonal, square, and hexagonal rings. On the other hand, larger metal encapsulated silicon cage structure ($N > 16$) is rarely reported in experiments.[21]

Due to the lack of experimental evidence of silicon fullerene cages, it is thus interesting to consider whether the silicon fullerene cages can be stabilized by endohedral metal atoms. Recently, two theoretical results on metal encapsulated silicon fullerenes, $Th@Si_{20}$ (I_h) (Ref. 18) and $M_4@Si_{28}$ (T_d, M=Al, Ga) (Ref. 19), have been reported. In these endohedral fullerene structures, perfect silicon fullerene cages of Si_{20} and Si_{28} can be stabilized by specific metal atom/cluster species encapsulated. The idea behind the molecular design of these two silicon fullerene clusters is due to two aspects. For $Th@Si_{20}$, the electron transfer from the central Th atom to the Si_{20} cage results in extra stabilization of the outer cage,[18,22] whereas the stability of $M_4@Si_{28}$ (M=Al, Ga) is due in part to the great aromaticity of inner close packed metal cluster (M_4).[19,22] A recent study, however, showed that $Th@Si_{20}$ (I_h) had imaginary frequencies,[22] suggesting that $Th@Si_{20}$ entailed lower symmetry than I_h. To our knowledge, the $M_4@Si_{28}$ (M

[a)]Electronic mail: xczeng@phase2.unl.edu

TABLE I. Effect of basis sets on the calculated properties of fullerene like $Si_{20}Pt_{10}$ (PBE1PBE functional).

Properties	6-31G(d) and LANL2DZ	6-311+G(d,p) and SDD
r_{Si-Si} (Å)	2.35 and 2.31	2.35 and 2.31
r_{Si-Pt} (Å)	2.30	2.29
Point group	D_{5d}	D_{5d}

=Al, Ga) cluster is perhaps the only stable silicon fullerene whose Si_{28} cage retains the same point-group symmetry (T_d) as homologous carbon fullerene C_{28} (T_d).

Sun *et al.* attempted to stabilize the Si_{60} fullerene cage using a C_{60} core. They have found that the Si_{60} cage tends to break the I_h symmetry and to relax into a distorted structure even with the encapsulated species.[11] We also made some effort to stabilize silicon fullerene Si_{60} by encapsulating metal clusters that have icosahedral symmetry. However, none of these attempts were successful due to the lack of encapsulated species (core) that can be exactly fitted into the fullerene cage (shell). Until now, we are unaware of any report on the stabilization of Si_{60} (I_h) structure via encapsulation. On the other hand, successful attempts have been made via molecular design of carbon-doped $Si_{60}C_{2n}$ (n =1,2),[23] exohedral hydrogen silicon fullerenes,[24,25] and silica (SiO_2) coated[26] silicon fullerenes.

In this work, we propose a new ligand strategy which uses exohedral transition metal atoms, platinum (Pt), to fully stabilize the silicon fullerene structures. This ligand strategy allows a whole class of silicon fullerene cages, with the number of skeleton atoms N from 20 to 60 (N=20, 24, 26, 28, 30, 32, 36, 42, 50, and 60), to be fully stabilized by $N/2$ exohedral Pt atoms. Here, the exohedral silicon fullerene is denoted as $Si_NPt_{N/2}$.

COMPUTATIONAL MODEL AND METHOD

All initial fullerene structures of $Si_NPt_{N/2}$ are constructed based on the skeleton of their carbon fullerene counterparts.[27] The Pt atoms are placed above the Si–Si bonds to generate the initial structures.

The density functional theory (DFT) calculations are performed using both DMOL3 (Ref. 28) and GAUSSIAN03 (Ref. 30) packages. The preoptimizations of $Si_NPt_{N/2}$ clusters are performed using the generalized gradient approximation (GGA) with the Perdew-Burke-Ernzerhof (PBE)[29(a)] functional implemented in the DMOL3 package. The d-polarization function included double-numerical basis set is adopted. The obtained structures of $Si_NPt_{N/2}$ from DMOL3 are further optimized using GAUSSIAN03 package.[30] The hybrid functional PBE1PBE is adopted for the optimization without geometrical constraint. The 6-31G(d) and effective core potential LANL2DZ basis sets[31] are applied to the silicon and platinum atoms, respectively. It is found that these basis sets provide a compromise between computational efficiency and accuracy (see Table I). The effect of functional on the calculation results is examined for $Si_{20}Pt_{10}$, $Si_{24}Pt_{12}$, $Si_{26}Pt_{13}$, and $Si_{60}Pt_{30}$ (Tables II and III). For the smallest $Si_{20}Pt_{10}$ cluster, we find that the hybrid functional (PBE1PBE,[29(a)] MPW1PW91,[29(b)] and B3LYP[29(c)]) and GGA functional (PBEPBE,[29(a),29(d)] BP86,[29(e),29(f)] and BLYP[29(e)–29(g)]) yield different predictions on the stabilities of the clusters, but all functionals do give consistent prediction of the stabilities of $Si_NPt_{N/2}$ for $N>24$.

RESULTS AND DISCUSSION

Figure 1 presents optimized structures of $Si_NPt_{N/2}$ (N=20, 24, 26, 28, 30, 32, 36, 42, 50, and 60). These structures are further confirmed to be true *local* minima by frequency calculations. Other properties such as symmetry, relative stabilities, and binding energy of $Si_NPt_{N/2}$ clusters are listed in Table III.

The smallest cluster reported here is $Si_{20}Pt_{10}$. For the ideal I_h symmetrical Si_{20}, the icosahedral cage has slightly protuberant geometry. That is, the bonding within the cage becomes much sp^3 like. Imposed by exohedral platinum atoms, the $Si_{20}Pt_{10}$ reduces symmetry to the D_{5d}. As shown in Fig. 1, the optimized $Si_{20}Pt_{10}$ and its inner Si_{20} cage both keep symmetries in the D_{5d} point group. Two Si–Si bond lengths, 2.31 and 2.35 Å, are detected in the inner Si_{20} cage. However, the $Si_{20}Pt_{10}$ structure may be not a true local minimum. As shown in Tables II and III, our calculations with different functional give contradicting predictions on the stability of the $Si_{20}Pt_{10}$. The calculations based on the hybrid functional PBE1PBE (see Table III)[29(a)] MPW1PW91,[29(b)] B3LYP,[29(c)] and the functional BLYP[29(e)–29(g)] within GGA all suggest that $Si_{20}Pt_{10}$ is a true local minimum without imaginary frequency. However, other GGA functionals including PBEPBE[29(a),29(d)] and BP86[29(e),29(f)] show that the fullerene-like $Si_{20}Pt_{10}$ has two imaginary frequencies (Table II).

For the larger $Si_NPt_{N/2}$ (N=24, 26, 28, 30, 32, 36, 42, 50, and 60), all structures represent true local minima. For example, the optimized structures of $Si_{24}Pt_{12}$, $Si_{26}Pt_{13}$ as well as $Si_{60}Pt_{30}$ are also examined using both PBE1PBE[29(a)] and PBEPBE[29(a),29(d)] functionals (Table II). Similar to the $Si_{20}Pt_{10}$, larger $Si_NPt_{N/2}$ with the number of silicon atom (N)

TABLE II. The lowest frequencies (in cm^{-1}) of $Si_NPt_{N/2}$ calculated via different functionals. [The basis set is 6-31G(d) for silicon and LANL2DZ for platinum.] The labels are according to Fowler and Manolopoulos (Ref. 27 in text).

	MPW1PW91	B3LYP	PBEPBE	BLYP	BP86
$Si_{20}Pt_{10}$	27.5	29.1	−65.2, −61.2	26.5	−30.9, −27.3
$Si_{24}Pt_{12}$	⋯	29.3	15.9	⋯	⋯
$Si_{26}Pt_{13}$	⋯	29.7	21.9	27.02	22.83
$Si_{60}Pt_{30}$	⋯	⋯	18.6 (I_h)	⋯	⋯

TABLE III. The symmetries (with/without exohedral platinum atoms), HOMO-LUMO gaps (eV), energy difference between isomers (ΔE), bond lengths of Si–Si ($r_{\text{Si–Si}}$), binding energies (BE_{whole} and BE_{part}), and lowest frequencies (by the PBE1PBE [Ref. 29(a)] functional) of $Si_NPt_{N/2}$, and comparison with their carbon fullerene counterparts (values in parentheses and text in italics).

$Si_NPt_{N/2}$	Label[a]	Sym.[b]/Sym.[c]	$E_{\text{HOMO-LUMO}}$ (eV)	ΔE (eV)	($r_{\text{Si–Si}}$) (Å)	BE_{whole}/BE_{part} (eV)	Lowest frequency by PBE1PBE (cm^{-1})
$Si_{20}Pt_{10}$	*I_h*	D_{5d}/D_{5d}	1.31 (*1.94*)	⋯	2.31, 2.35	4.89/3.41	26.5
$Si_{24}Pt_{12}$	*D_{6d}*	D_{2d}/D_{6d}	1.43 (*2.07*)	⋯	2.31–2.36	4.91/3.46	26.6
$Si_{26}Pt_{13}$	*D_{3h}*	C_{2v}/C_{2v}	1.77 (*1.95*)	⋯	2.32–2.35	4.93/3.52	27.0
$Si_{28}Pt_{14}$	*T_d*	D_{2d}/D_{2d}	2.01 (*1.52*)	0.0 (*0.0*)	2.30–2.37	4.95/3.58	24.9
	D_2	C_1/C_1	1.51 (*1.88*)	0.69 (*0.30*)	2.31–2.36	4.93/3.53	28.2
	cc1	C_{2v}/C_{2v}	1.46 (*1.73*)	1.16 (*2.44*)	2.30–2.36	4.92/3.50	22.1
$Si_{30}Pt_{15}$	*cc2*	C_{2v}/C_{2v}	1.39 (*1.59*)	0.33 (*0.19*)	2.31–2.36	4.94/3.55	23.0
	cc3	C_{2v}/C_{2v}	1.71 (*1.63*)	0.0 (*0.0*)	2.31–2.35	4.95/3.57	25.2
$Si_{32}Pt_{16}$	*cc2*	C_2/C_2	1.33 (*1.62*)	⋯	2.30–2.37	4.93/3.53	23.7
	cc12	C_1/C_1	1.47 (*1.69*)	0.31 (*0.29*)	2.31–2.36	4.95/3.60	26.0
$Si_{36}Pt_{18}$	*cc14*	C_{2v}/C_{2v}	1.65 (*1.61*)	0.0 (*0.0*)	2.31–2.35	4.96/3.62	24.8
	cc15	C_{2h}/C_{2h}	1.56 (*1.29*)	0.39 (*0.16*)	2.31–2.35	4.95/3.60	26.4
	cc32	C_1/C_1	1.63 (*1.70*)	0.31 (*1.13*)	2.31–2.35	4.97/3.66	23.7
$Si_{42}Pt_{21}$	*cc33*	C_1/C_1	1.58 (*1.75*)	0.40 (*1.14*)	2.31–2.35	4.97/3.65	25.3
	cc45	D_3/D_3	1.55 (*2.23*)	0.0 (*0.0*)	2.30–2.35	4.98/3.67	23.3
$Si_{50}Pt_{25}$	*cc271*	C_{2v}/C_{2v}	1.94 (*1.50*)	⋯	2.31–2.35	5.00/3.73	23.9
$Si_{60}Pt_{30}$	*cc1812*[d]	C_1/I_h	2.22 (2.88)	0.0	2.32, 2.34	5.01/3.75	23.6
	cc1812[d]	I_h/I_h	2.27 (2.88)	0.01	2.32, 2.34	5.01/3.75	23.1

[a]The labels are according to Fowler and Manolopoulos for homologous carbon fullerenes (Ref. 27)
[b]Symmetries of optimized $Si_NPt_{N/2}$.
[c]Symmetries of core silicon cage (Si_N).
[d]IPR structure.

varied from 24 to 50 generally has lower symmetries, compared to core Si fullerene structures, as shown in Table III and Fig. 1. However, geometrical analysis suggests that the core silicon fullerene cages Si_N ($N=24,26,28,30,32,36,42,50$) only undergo small structural distortions, compared to perfect fullerene structures. The lengths of Si–Si bonds in the $Si_NPt_{N/2}$ ($N=24-50$) are within the range of 2.30–2.37 Å, comparable to previously reported 2.27–2.36 Å in the fullerenelike M@Si_{16} (M=Ti, Sc, etc.).[14]

The $Si_{60}Pt_{30}$ is distinguished from other $Si_NPt_{N/2}$ ($N=24-50$) structures by its highest I_h symmetry. The I_h symmetry is retained with 30 platinum atoms exohedrally bounded onto the Si_{60}. As shown from previous theoretical studies, the optimized Si_{60} itself cannot keep I_h symmetry as the buckyball C_{60}.[11] After DFT optimizations, two isomers with C_1 and I_h symmetries are presently obtained for the $Si_{60}Pt_{30}$. The geometries of exohedral Pt coating in the C_1 symmetrical $Si_{60}Pt_{30}$ are slightly distorted in comparison with I_h symmetrical $Si_{60}Pt_{30}$. The two isomers are almost isoenergetic because the C_1 symmetrical $Si_{60}Pt_{30}$ is only 0.01 eV lower in energy than the I_h symmetrical $Si_{60}Pt_{30}$. The frequency calculations show that these two isomer structures are local minima with the lowest frequencies being 23.6 cm^{-1} (C_1 symmetrical) and 23.1 cm^{-1} (I_h symmetrical), respectively (see Table III). The slight split of the frontier-orbital energy level is found in the C_1 symmetrical $Si_{60}Pt_{30}$ (Fig. 2). It is interesting to note that the silicon fullerene cage (Si_{60}) in either the C_1 or I_h symmetrical $Si_{60}Pt_{30}$ exhibits perfect I_h symmetry. The bond length of Si–Si in the inner Si_{60} cage varies between 2.32 and 2.34 Å.

In contrast to the core Si fullerene cages, the exohedral Pt-coated silicon fullerenes ($Si_NPt_{N/2}$, $20 \leqslant N \leqslant 60$) possess relatively higher stabilities. It can be seen in Fig. 2 that the highest occupied molecular orbital-lowest unoccupied molecular orbital (HOMO-LUMO) gap of the Si_{60} increases significantly (~0.8 eV) with exohedrally binding Pt atoms. As shown in Table III, the calculated values of for $Si_NPt_{N/2}$ are in the range of 1.31–2.27 eV. Among them, the $Si_{60}Pt_{30}$ has the largest HOMO-LUMO gaps, 2.22 (C_1) and 2.27 (I_h) eV. The $Si_{20}Pt_{10}$ has the smallest HOMO-LUMO gap (~1.31 eV). Because the hybrid functional such as PBE1PBE may overestimate the HOMO-LUMO gap,[32] we also examined HOMO-LUMO gaps of carbon fullerenes using the same level of theory. In Table III, it can be seen that the HOMO-LUMO gaps of $Si_NPt_{N/2}$ are comparable to those of carbon fullerenes. Among them, the $Si_{60}Pt_{30}$ and $Si_{28}Pt_{14}$ have HOMO-LUMO gaps exceeding 2.0 eV, implying relatively high chemical stability of the $Si_{60}Pt_{30}$ and $Si_{28}Pt_{14}$. In general, the HOMO-LUMO gap of $Si_{60}Pt_{30}$ is lower than that of carbon fullerene C_{60} by about 0.6 eV (see Table III).

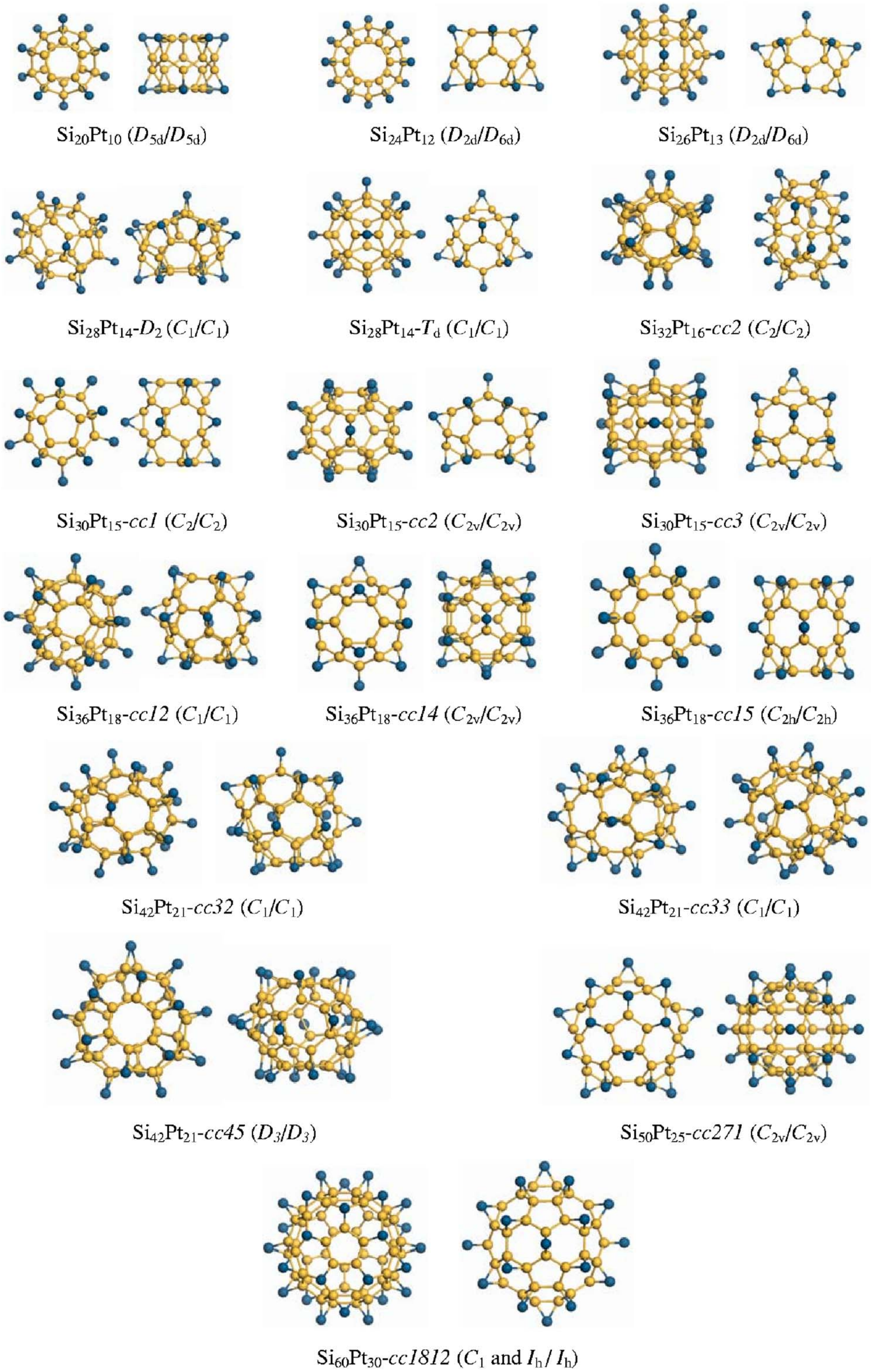

FIG. 1. (Color online) Top and side views of optimized cluster $Si_NPt_{N/2}$. The labels are according to Fowler and Manolopoulos for homologous carbon fullerenes (Ref. 27). Point groups of optimized structures ($Si_NPt_{N/2}$/Si_N core) are given in parenthesis. Yellow/blue spheres represent silicon/platinum atoms.

However, the HOMO-LUMO gap of D_{2d} symmetrical $Si_{28}Pt_{14}$ (~2.01 eV) is actually higher than that of C_{28} (T_d) by ~0.5 eV.

The stabilities of exohedral Pt-coated silicon fullerenes are mainly attributed to the Pt atoms ($Pt_{N/2}$). Differing from carbon fullerenes, no apparent electron delocalization is found in $Si_NPt_{N/2}$ clusters. The spherical aromaticity of certain $Si_NPt_{N/2}$ is evaluated through calculating the nucleus-independent chemical shift (NICS)[33] values. Here, the NICS values of $Si_{20}Pt_{10}$, $Si_{28}Pt_{14}$, and $Si_{60}Pt_{30}$ are 13.2, 2.1, and −5.5, respectively, implying that the aromatic stabilization contributes little to the stability of cages. It is known that transition metal atoms with 4*d* and 5*d* valence electrons are capable of forming η^2-disilene complexes with the disilene compound, in which the transition metal atom binds to the silicon "double" bond through the σ-π interaction.[34] For the disilene, the binding energy of platinum atom to Si=Si bond is ~7 eV [PBE1PBE/6-311+g(d,p) for Si and LANL2DZ for Pt]. The bonding mechanism can be described by the Dewar-Chatt-Duncanon picture (Fig. 3): the

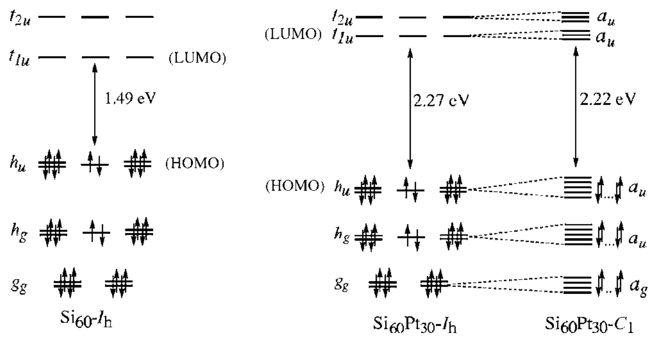

FIG. 2. Comparisons of frontier-orbital energy levels of Si_{60} (I_h) and $Si_{60}Pt_{30}$ (in I_h and C_1 symmetries) calculated using the PBE1PBE functional.

π-type orbital (HOMO) on the Si=Si bond donating electrons to the empty metal orbital and the π^* orbital of disilene could be involved in back donation from the d_π metal orbital.[35] The silicon fullerene cages have curved Si–Si bonds analogous to the Si=Si double bond of the disilene. The Pt atoms ($Pt_{N/2}$) can bind to the Si–Si bond tightly, depleting excess dangling bonds of the silicon fullerene cages (Si_N), thereby enhancing the stabilities of fullerene cages. In fact, besides the Pt atom, most of 4*d* and 5*d* transition metal atoms in the Periodic Table (such as Pd, Au, Ti, and Zr) are also expected to stabilize silicon fullerene cages. However, only $Si_NPt_{N/2}$ cluster is found to be true local minima (calculations using the PBE1PBE and PBEPBE functional). This result is somewhat surprising since Pt has nearly fully occupied 5*d* orbital. The reason for Pt being the only transition metal to stabilize silicon fullerenes is unclear. At present, we speculate that the strong relativistic effect of the Pt atom might contribute further to such stabilizations.

Binding energies (BEs) of $Si_NPt_{N/2}$ are evaluated. Two forms of BEs, BE_{whole} and BE_{part}, defined below are calculated:

$$BE_{whole} = -[E_{(Si_NPt_{N/2})} - (N/2)E_{(Pt)} - NE_{(Si)}]/1.5N, \quad (1)$$

$$BE_{part} = -[E_{(Si_NPt_{N/2})} - (N/2)E_{(PtSi_2)}]/(N/2). \quad (2)$$

As for the BE_{part}, we assume the formation process for the $Si_NPt_{N/2}$ such that (1) the platinum atom binds two silicon atoms at first, forming a $PtSi_2$ structural unit, and then (2) the $PtSi_2$ units resemble into small structural motifs and further into cluster $Si_NPt_{N/2}$. This process of formation is analogous to the proposed fragment growth mechanism of C_{60}, which involves a series subgrowth process from small carbon fragments.[1] We emphasize that the binding energy of Pt atom to the Si=Si double bond (~7.0 eV by PBE1PBE with the

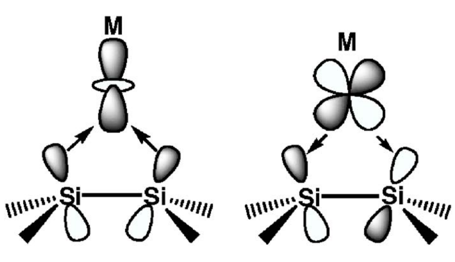

FIG. 3. Bonding picture between transition metal atom (M) and the Si=Si double bond.

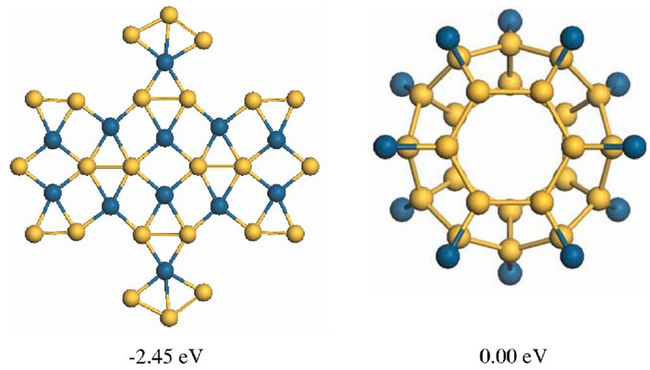

FIG. 4. (Color online) Relative stabilities of nonfullerene and fullerene isomers of $Si_{24}Pt_{12}$. The silicon and platinum atoms are in yellow and blue colors, respectively.

disilene model) is much larger than the cohesive energy (~5.9 eV) (Ref. 36) of bulk Pt, suggesting that the formation of $Si_NPt_{N/2}$ will be energetically much more favorable than the self-clustering of Pt atoms. The calculated binding energies, BE_{whole} and BE_{part}, are given in Table III. The values of BE_{whole} are much larger than those of BE_{part} because of large binding energies contributed by the attachment of Pt atom to the Si=Si species. The calculated BE_{part} is in the range of 3.41–3.75 eV, among which the $Si_{60}Pt_{30}$ has largest binding energy (3.75 eV). The binding energies of $Si_NPt_{N/2}$ are close to experimental measurements of pure silicon clusters with similar sizes,[37] providing further evidences on relatively high stability of $Si_NPt_{N/2}$ clusters. Furthermore, the relative stabilities of isomers of $Si_NPt_{N/2}$ are compared with their carbon fullerene counterparts (C_N). To this end, the relative stabilities of some energetically low-lying isomers of $Si_{28}Pt_{14}$, $Si_{30}Pt_{15}$, $Si_{36}Pt_{18}$, as well as $Si_{42}Pt_{21}$ are calculated and compared with their carbon fullerene counterparts: C_{28}, C_{30}, C_{36}, and C_{42}. The data in Table III show the low-energy structures of sampled $Si_NPt_{N/2}$ and C_N ($N=28,30,36,42$) with the same cage skeletons. Interestingly, we find that the trends in relative stabilities among isomers of $Si_{28}Pt_{14}$, $Si_{30}Pt_{15}$, and $Si_{42}Pt_{21}$ are consistent with those of C_{28}, C_{30}, and C_{42}, respectively (see Table III). Only minor inconsistency in stability trend is found among isomers of $Si_{36}Pt_{18}$ and C_{36}.

Finally, we note that the present $Si_NPt_{N/2}$ fullerene structures all correspond to local minima, largely because the exohedral Pt atoms on the $Si_NPt_{N/2}$ clusters are not fully saturated. The platinum atom generally forms planar four-coordinate complex binding by ligands.[38] Indeed, a nonfullerene planarlike isomer of $Si_{24}Pt_{12}$ (Fig. 4) in which all Pt atoms have four-coordination with Si atoms gives appreciably lower energy (2.45 eV) than the fullerene structure. Hence, the freestanding fullerenelike $Si_NPt_{N/2}$ are only metastable due to the unsaturated Pt atoms. However, our main point here is that the *inner* silicon fullerene cage can be fully stabilized by the exohedral Pt coating. If additional ligands such as $-PH_3$, –Cl, etc., are further introduced to saturate the exohedral Pt atoms, the inner fullerenelike $Si_NPt_{N/2}$ cluster can be fully stabilized. For example, a $[(PH_3)_2Pt]$ can be viewed as a ligand unit that can bind to two silicon atoms. An optimized structure $Si_{24}[(PH_3)_2Pt]_{10}$ is illustrated in Fig. 5, which contains silicon fullerene Si_{24}

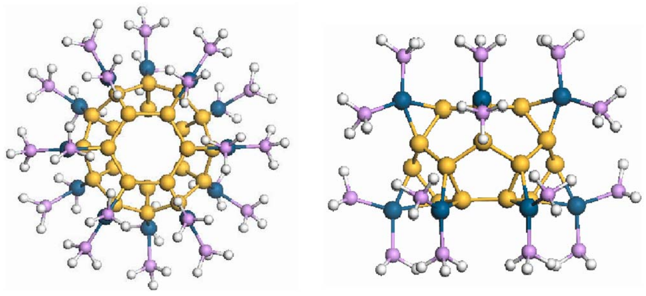

FIG. 5. (Color online) Top and side views of optimized $-PH_3$ ligand stabilized $Si_{24}Pt_{12}$ fullerene structure, $Si_{24}[(PH_3)_2Pt]_{10}$. The silicon, platinum, phosphorus, and hydrogen atoms are in yellow, blue, pink, and white colors, respectively.

stabilized by the $[(PH_3)_2Pt]_{10}$. The introduction of molecular ligands to saturate exohedral Pt atoms may be a more realistic way to isolate exohedral silicon fullerene clusters.[4]

CONCLUSION

In summary, we propose a molecular design to stabilize the silicon fullerene cages ($Si_{24}-Si_{60}$) by exohedrally coating Pt atoms. The exohedral silicon fullerenes $Si_NPt_{N/2}$ are found to be *local* minima and possess large HOMO-LUMO gaps close to their carbon fullerenes counterparts (C_N). In particular, the silicon buckminsterfullerene Si_{60} can be fully stabilized by 30 exohedral Pt atoms to retain I_h symmetry as C_{60}. The HOMO-LUMO gap (~2.27 eV) and binding energy (3.75 eV) of the $Si_{60}Pt_{30}$ are both the highest among the currently studied $Si_NPt_{N/2}$ clusters. It is worthy to note that many $Si_NPt_{N/2}$ clusters have nearly the same trend in relative stability among their fullerene isomers as that of homologous carbon fullerenes (C_N). Finally, the introduction of molecular ligands to saturate exohedral Pt atoms may be a more realistic way to isolate exohedral silicon fullerene clusters. It is our hope that the present study can stimulate further experimental exploration of exohedral silicon fullerene structures. If successful, the hollow space inside the silicon fullerenes is capable of accommodating guest species, such as small metal clusters, which may offer interesting chemistry analog to endohedral metallofullerenes.[39,40]

ACKNOWLEDGMENTS

This work was supported by grants from the DOE Office of Basic Energy Sciences (DE-FG02-04ER46164), National Science Foundation (CHE-0427746 and CHE-0701540), the Nebraska Research Initiative, and by the UNL Research Computing Facility.

[1] G. S. Hammond and V. J. Kuck, *Fullerenes: Synthesis, Properties, and Chemistry of Large Carbon Clusters*, ACS Symposium Series 481 (American Chemical Society, Washington, DC, 1991).
[2] H. W. Kroto, J. R. Heath, S. C. O'Brien, R. F. Curl, and R. E. Smalley, Nature (London) **318**, 162 (1985).
[3] W. Kratschmer, L. D. Lamb, K. Fostiropoulos, and D. R. Huffman, Nature (London) **347**, 354 (1990).
[4] J. F. Bai, A. V. Virovets, and M. Scheer, Science **300**, 781 (2003).
[5] S. Bulusu, X. Li, L.-S. Wang, and X. C. Zeng, Proc. Natl. Acad. Sci. U.S.A. **103**, 8326 (2006).
[6] P. W. Fowler, T. Heine, D. Mitchell, R. Schmidtb, and G. Seifert, J. Chem. Soc., Faraday Trans. **92**, 2197 (1996).
[7] C. Liang and L. C. Allen, J. Am. Chem. Soc. **112**, 1039 (1990).
[8] J. Dabrowski and H.-J. Müssig, *Silicon Surfaces and Formation of Interfaces* (World Scientific, Singapore, 2003).
[9] R. R. Hudgins, M. Imai, M. F. Jarrold, and P. J. Dugourd, J. Chem. Phys. **111**, 7865 (1999).
[10] M. F. Jarrold and V. A. Constant, Phys. Rev. Lett. **67**, 2994 (1991).
[11] Q. Sun, Q. Wang, P. Jena, B. K. Rao, and Y. Kawazoe, Phys. Rev. Lett. **90**, 135503 (2003).
[12] S. Yoo, J. J. Zhao, J. L. Wang, and X. C. Zeng, J. Am. Chem. Soc. **126**, 13845 (2004).
[13] H. Hiura, T. Miyazaki, and T. Kanayama, Phys. Rev. Lett. **86**, 1733 (2001).
[14] V. Kumar and Y. Kawazoe, Phys. Rev. Lett. **87**, 045503 (2001).
[15] Q. Sun, Q. Wang, T. M. Briere, V. Kumar, and V. Kawazoe, Phys. Rev. B **65**, 235417 (2002).
[16] J. Lu and S. Nagase, Phys. Rev. Lett. **90**, 115506 (2003).
[17] K. Koyasu, M. Akutsu, M. Mitsui, and A. Nakajima, J. Am. Chem. Soc. **127**, 4998 (2005).
[18] A. K. Singh, V. Kumar, and Y. Kawazoe, Phys. Rev. B **71**, 115429 (2005).
[19] Y. Gao and X. C. Zeng, J. Chem. Phys. **123**, 204325 (2005).
[20] J. M. Goicoechea and S. C. Sevov, J. Am. Chem. Soc. **127**, 7676 (2005).
[21] S. Yamanaka, E. Enishi, H. Fukuoka, and M. Yasukawa, Inorg. Chem. **39**, 56 (2000).
[22] Z. Chen, S. Neukermans, X. Wang, E. Janssens, Z. Zhou, R. E. Silverans, R. B. King, P. v. R. Schleyer, and P. Lievens, J. Am. Chem. Soc. **128**, 12829 (2006).
[23] A. Srinivansan, M. N. Huda, and A. K. Ray, Phys. Rev. A **72**, 063201 (2005).
[24] F. Pichierri, V. Kumar, and Y. Kawazoe, Chem. Phys. Lett. **383**, 544 (2004).
[25] A. J. Karttunen, M. Linnolahti, and T. A. Pakkanen, J. Phys. Chem. C **111**, 2545 (2007).
[26] D. Zhang, G. Guo, and C. Liu, J. Phys. Chem. B **110**, 14619 (2006).
[27] P. W. Fowler and D. E. Manolopoulos, *An Atlas of Fullerenes* (Clarendon, Oxford, 1995).
[28] B. Delley, J. Chem. Phys. **92**, 508 (1990); **113**, 7756 (2003); DMol3 is available from Accelrys.
[29] (a) J. P. Perdew, K. Burke, and M. Ernzerhof, Phys. Rev. Lett. **77**, 3865 (1996); (b) C. Adamo and V. Barone, J. Chem. Phys. **108**, 664 (1998); (c) A. D. Becke, *ibid.* **98**, 5648 (1993); (d) J. P. Perdew, K. Burke, and M. Ernzerhof, Phys. Rev. Lett. **78**, 1396 (1997); (e) A. D. Becke, Phys. Rev. A **38**, 3098 (1988); (f) J. P. Perdew, Phys. Rev. B **33**, 8822 (1986); (g) C. Lee, W. Yang, and R. R. Parr, *ibid.* **37**, 785 (1988); (h) B. Miehlich, A. Savin, H. Stoll, and H. Preuss, Chem. Phys. Lett. **157**, 200 (1989).
[30] M. J. Frisch, G. W. Trucks, H. B. Schlegel *et al.*, GAUSSIAN 03, Revision C.02, Gaussian, Inc., Wallingford, CT, 2004.
[31] W. R. Wadt and P. J. Hay, J. Chem. Phys. **82**, 284 (1985).
[32] G. Zhang and C. B. Musgrave, J. Phys. Chem. A **111**, 1154 (2007).
[33] P. V. R. Schleyer, C. Maerker, A. Dransfeld, H. Jiao, and N. J. R. van Eikema Hommes, J. Am. Chem. Soc. **118**, 6317 (1996).
[34] E. K. Pham and R. West, J. Am. Chem. Soc. **111**, 7667 (1989); Organometallics **9**, 1517 (1990).
[35] R. Konecny and R. Hoffmann, J. Am. Chem. Soc. **121**, 7918 (1999).
[36] C. Kittel, *Introduction to Solid State Physics* (Wiley, New York, 1986).
[37] T. Bachels and R. Schafer, Chem. Phys. Lett. **324**, 365 (2000).
[38] J. J. MacDougall, J. H. Nelson, and F. Mathey, Inorg. Chem. **21**, 2145 (1982).
[39] H. Shinohara, Rep. Prog. Phys. **63**, 843 (2000).
[40] *Endofullerenes: A New Family of Carbon Clusters*, edited by T. Akasaka and S. Nagase (Kluwer Dordrecht, 2002).